Far infrared solar physics

G. Trottet and K.-L. Klein

Observatoire de Paris, LESIA-CNRS UMR 8109, Univ. P & M Curie and Paris-Diderot, Observatoire de Meudon, 92195 Meudon, France
e-mail: `gerard.trottet@obspm.fr`

Abstract. Measurements of the far infrared (FIR) continuum from stratospheric balloons or aircraft have addressed the temperature structure of the solar chromosphere in both the quiet Sun and non-flaring active regions. Although submillimeter observations of flares have been obtained over the past ten years, the infrared spectrum of solar flares is still unknown over a wavelength range of more than two orders of magnitude. We outline that spectral and imaging measurements in the FIR continuum, which extend those obtained at submillimeter wavelengths, constitute new key diagnostics of processes relating to the acceleration of relativistic electrons and ions and to the energy transport and deposition in flares. We briefly describe pioneer instrumental concepts studied to open the FIR domain to flare observations. Finally we emphasize the need of a future solar-dedicated mission, performing joint spectral and imaging observations from the FIR domain to high energy gamma-rays, in order to get a complete picture of particle acceleration and energy transport during flares.

Key words. Sun: infrared – Sun: flares – Sun: atmosphere – Sun: radio radiation

1. Introduction

The far infrared (FIR) solar continuum (0.5-20 THz) is an excellent thermometer for most of the photosphere and for the chromosphere. It has thus played an important role in the modeling of the low chromosphere and temperature minimum region. An extensive review of FIR continuum observations and results addressing the temperature and density structure of the quiet atmosphere has been presented in Deming et al. (1991). Briefly stated these observations clearly show the existence of a temperature minimum, provide evidence for limb brightening indicating that the structure of the chromosphere is far to be smooth even at the lowest levels, and reveal the 5-minute oscilla-

Send offprint requests to: G. Trottet

tions which are almost entirely caused by temperature variations in the atmospheric medium associated with them. FIR imaging from a balloon-borne telescope have shown temperature enhancements in active regions which are larger in the lower chromosphere than in the upper photosphere (Degiacomi et al. 1985).

No observations exist so far of the FIR continuum during solar flares though the interest to perform such measurements has long been emphasized (Ohki & Hudson 1975). Such measurements are difficult because of the high background emission of the quiet Sun and non flaring active regions. Nevertheless, the need of FIR observations of flares is further demonstrated by radio measurements obtained in the 200-400 GHz range over the past ten years . In particular these observations have revealed an
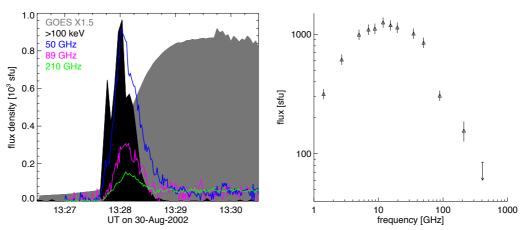
Fig. 1. Left: Radio flux densities (1sfu=10^{-22}Wm^{-1}Hz^{-1}) at different frequencies. Right: radio spectrum during peak time.The smooth grey and the black curves in the left represent respectively the time evolution of the 1-8 Å soft X-rays and > 100 keV hardX-rays. (From Krucker et al. (2012))

unexpected upturn of the flare spectrum at sub-THz frequencies which cannot be satisfactory understood without photometric and imaging measurements in the FIR domain.

The goal of this report is to present key scientific questions the answer to which need new diagnostics provided by FIR measurements of the continuum during solar flares. In the first section we give a brief overview of the 200-400 GHz observations of flares and of the different interpretations proposed. Section 3 reports scientific objectives indicating why to observed flares in the FIR domain. In section 4 we present pioneer instrumental concepts for flare observations at THz frequencies. The final section gives a summary and emphasizes the need of a solar dedicated space mission concept combining FIR measurements with UV/EUV, soft and hard X-rays, and high-energy gamma-rays.

2. Observations of solar flares in the 200-400 GHz domain

Total flux measurements of solar flares have been performed for decades in the microwave domain at fixed frequencies between 1 and 90 GHz. The observed radio bursts generally consist in a rapidly varying emission lasting for a few minutes referred to below as impulsive bursts. For some events this initial impulsive

emission is followed by a time-extended (tens of minutes and more) emission referred to below as gradual bursts. The emission mechanism of microwave impulsive bursts is well explained by incoherent gyrosynchrotron emission from electrons with energies between a few hundred of keV and some MeV moving through magnetic fields of typically 100-1000 G above active regions (Pick, Klein & Trottet 1990; Bastian, Benz & Gary 1998). Gradual microwave bursts are, at least partly, due to thermal free-free emission from coronal sources at a few 10^6 K (White & Kundu 1992).

New instrumentation observing in the 200–400 GHz range became available in year 2000. Since then, these observations have been routinely performed by the Solar Sub-millimeter Telescope (SST) at 212 and 405 GHz (Kaufmann et al. 2001). Observations have also been obtained during short campaigns at 230 and 345 GHz by the KOSMA (Köln Observatory for Submillimeter and Millimeter Astronomy) telescope, and at 210 GHz by BEMRAK (BErnese Multibeam RAdiometer for KOSMA, Lüthi et al. (2004a); Lüthi et al. (2004b)). Both, SST at 212 GHz and BEMRAK at 210 GHz, provide multi-beam measurements that allow to estimate the location (center of mass) and the overall size of the millimeter-wave emitting region. The ensem-

ble of these new observations has been critically and extensively discussed in Krucker et al. (2012). Radio events observed in the 200-400 GHz domain can be classified into three types: normal, THz and gradual events. For each of these three categories of 200-400 GHz events, we give below a brief summary of the characteristics of the radio emission and indicate which emission mechanisms have been proposed.

2.1. Normal events

The left panel in Fig. 1 displays the time variations of the radio flux densities at different frequencies and of the soft X-ray and hard X-ray emissions during a X1.5 flare that occurred on August 30, 2002. This event was clearly detected by SST at 212 GHz, but only an upper limit of the flux density could be estimated at 405 GHz (Giménez de Castro et al. 2009). As in the microwave domain, there is a gross similarity between the time evolultions of the 212 GHz radio emission and of the > 100 keV hard X-rays. Figure 1 also shows the radio spectrum observed in the 1–400 GHz range around the maximum of the impulsive phase. This spectrum is reminiscent of the gyrosynchrotron emission from mildly relativistic electrons, commonly observed in the microwave domain with a spectral maximum between ~ 10 and 30 GHz. The emission in the 200-400 GHz range appears just to be the high-frequency extension of the gyrosynchrotron spectrum observed in the microwave domain. Other examples of normal events have been reported by (Trottet et al. 2002; Lüthi et al. 2004a; Trottet et al. 2011).

2.2. THz events

While normal events display a usual gyrosynchrotron spectrum during the impulsive phase, Fig 2 (right panel) shows an example of a radio spectrum which in addition to the microwave synchrotron spectrum exhibits a new component with increasing flux densities between 200 and 400 GHz . To emphasize the increasing spectra and the possibility that these events could be even more prominent in the THz range, we call these flares THz events. While normal events were associated with soft X-ray flares ranging from M-class to X6, the four events with the most distinct high-frequency components, detected so far, were large (X6 and higher), eruptive two ribbon events (Kaufmann et al. 2004; Lüthi et al. 2004b; Silva et al. 2007; Kaufmann et al. 2009). From the ratio of the time profiles at the two frequencies available, power-law slopes between 0.3 and 5 were derived (without any attempt to determine and subtract the normal gyrosynchrotron component observed at lower frequencies). It should be noted that, like for normal events, the time evolution of the 200-400 GHz radio emission is similar to that of the > 100 keV hard X-rays see Fig. 2(left).

Thermal free-free-emission is unlikely the emission mechanism of the THz component during the impulsive phase because it would require an extended emitting region (> 30″-40″) in the chromosphere. This is not observed at any other wavelengths, including hard X-rays which have similar time profiles as the THz radio component (Trottet et al. 2008; Krucker et al. 2012). Although only a few THz events have been reported so far, many non-thermal emission mechanisms have been proposed to explain the upturn of the radio spectrum in the 200-400 GHz domain. A detailed and critical discussion of these processes is beyond the scope of this report and can be found in (Krucker et al. 2012). Briefly stated, the proposed processes can be sorted into two categories: well-known and well-studied mechanisms and processes which need to be further studied. The former processes include: gyrosynchrotron emission from relativistic electrons and from relativistic positrons (Silva et al. 2007; Trottet et al. 2008), thermal synchrotron from coronal regions of extremely high magnetic field (few 1000 G) and temperature (> 10^8 K (Costa & Simões 2006) and inverse Compton scattering of microwave photons (Kaufmann et al. 1986). Processes that need to be further studied both theoretically and quantitatively include: diffusive radiation in Langmuir waves (Fleishman & Toptygin 2007), Cherenkov ra-
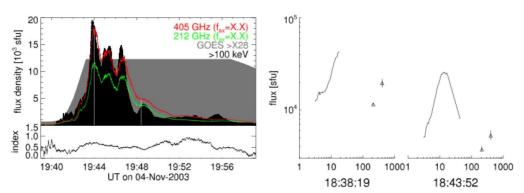
Fig. 2. Left: Radio flux densities at 212 and 405 GHz (upper curves) and power-law spectral index between 212 and 405 GHz (bottom curve). Right: Radio spectra at times marked by vertical white lines in the upper right panel. The smooth grey and the black curves in the left represent respectively the time evolution of the 1-8 Å soft X-rays and > 100 keV hard X-rays. (Adapted from Krucker et al. (2012))

diation (Fleishman & Kontar 2010), plasma radiation from electron beams (Sakai et al. 2006) and proton beams (Sakai & Nagasugi 2007a,b), coherent-bunch synchrotron radiation (Kaufmann & Raulin 2006) and synchrotron maser (Wu 1985; Louarn, Le Queau & Roux 1987). Even if it is not possible at present to state which process(es) is (are) the most likely to explain the THz component the following remarks have to be made:

- All mechanisms require extreme values for the parameters to which they are sensitive, e.g. extremely large number of electrons or positrons for non thermal synchrotron emission, too high temperatures and magnetic field strength for thermal synchrotron radiation.
- All mechanisms, except coherent-bunch radiation, predict that microwave and 200-400 GHz emitting regions are spatially different.
- Different mechanisms lead to different spectral shapes. For example: the gyrosynchrotron spectrum from a distinct population of high-energy electrons will show a marked peak somewhere above 400 GHz while that from positrons will show a flat maximum in the THz region and then decrease; diffusive radiation on Langmuir waves leads to a spectrum which falls abruptly above its maximum.

2.3. Gradual events

Figure 3 shows the time evolution of the soft X-ray emission detected in the GOES 0.1-0.8 nm channel and of the radio flux densities observed at 210, 230 and 345 GHz by BEMRAK and KOSMA and at 212 GHz by SST during a M6.7 flare that occurred on October 27, 2003. A detailed study of this flare has been presented in Trottet et al. (2011). The impulsive phase of this event (∼ 12:29-12:32 UT) is observed up to 345 GHz and belongs to the type of normal events discussed above. This impulsive phase is followed by a slowly varying and time extended phase which is more pronounced than the impulsive phase above 200 GHz. Its time evolution is similar to that of the soft X-ray emission. Figure 4 displays the mean radio spectrum measured between the two vertical dashed lines in Fig. 3 in the 1-345 GHz frequency range. The flat spectrum observed between 8 and 230 GHz is reminiscent of optically thin bremsstrahlung emission. Below 8 GHz the flux density decreases with decreasing frequency, indicating that the radio emitting source gradually becomes optically thick at low frequencies. The radio spectrum expected from an isothermal source of 40″diameter with emission measure and temperature derived from the soft X-ray measurements (dashed line in Fig. 4) is three to four times lower than the observed one. In addition to the emission from the hot (a few 10^7 K) soft
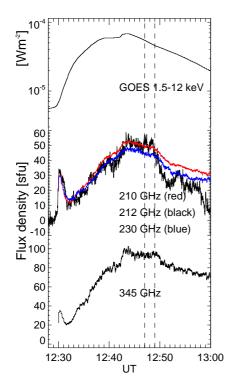
Fig. 4. Example of the radio spectrum observed during the time-extended (gradual) phase of the October 27, 2003 flare (asterisks with errors bars). The dashed lines indicate the radio spectrum expected purely from an isothermal plasma with temperature and emission measure derived from the GOES soft X-ray measurements, assuming a circular source of 40″ diameter, while the solid lines indicate the spectrum expected from a two-temperature model (see text).

Fig. 3. Time histories of X-ray and radio emissions during the October 27, 2003 flare at ~12:30 UT. From top to bottom: 1-8 Å soft X-ray flux (background subtracted) from the GOES-12 X-ray Sensor; radio flux densities at 210 GHz from BEMRAK (red), 230 GHz from KOSMA (blue), 212 GHz from SST (black), and at 345 GHz from KOSMA.

X-ray plasma, Trottet et al. (2011) have shown that, up to 230 GHz, the emission was predominantly radiated by a cooler coronal source at a temperature in the 1-3 10^6 K range. Indeed, the radio observations are well represented by the radio source model, shown by the solid line in Fig. 4, which includes the contributions of both a hot and a cool plasma..

Throughout the gradual phase, the 345 GHz flux density is significantly higher than that expected from the model that fits the flux densities measured in the 210-230 GHz range. The comparison with high cadence Hα and UV /EUV imaging observations led Trottet et al. (2011) to conclude that, at 345 GHz, in ad-
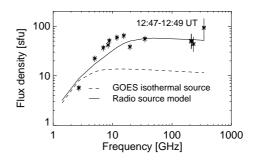
dition to the optically-thin coronal emission, there is an optically-thick component which for this flare was found to arise from the chromospheric Hα footpoints of a coronal loop system seen in EUV. Evidence for the contribution of chromospheric regions to the 200-400 GHz thermal radio emission have also been reported for other flares (Trottet et al. 2002; Lüthi et al. 2004a). For these events the 200-400 GHz emission is found to arise from large regions with diameters in the range 30″- 60″. There are also events, like for example the giant flare of 0ctober 28, 2003, where the gradual phase is predominantly radiated by gyrosynchrotron emission in the microwave domain and by optically-thick free-free emission at submillimeter wavelengths (Trottet et al. 2008).

The above discussion shows that radio observations at millimeter-submillimeter wavelengths constitute a unique tool to study the chromospheric response to flare energy during the gradual phase because the emission mechanism is well known and the radiative transport is simple.

3. Why to observe solar flares in the FIR domain?

The 200-400 GHz radio observations of flares discussed in the previous section emphasizes the need to obtain spectral and imaging measurements of the continuum emission in the say, 0.5-30 THz range, the last window of the solar spectrum which has not been studied yet. Future FIR observations will fill this gap and bring new insights relating to high-energy particles, the structure and dynamics of the flaring atmosphere and the mechanisms of energy transport during flares.

3.1. High-energy particles

Roughly speaking, an electron with a Lorentz factor γ radiates around a critical frequency (Pacholczyk 1970) $\nu_c \approx 1.5\gamma^2\nu_{ce}$ where ν_{ce} is the electron cyclotron frequency. Thus for a given magnetic field higher energy electrons radiate at higher frequencies. For normal events, the extrapolation of the gyro synchrotron spectrum from mildly relativistic electrons, observed up to 200-400 GHz, into the FIR domain should thus reveal that highly relativistic electrons have been accelerated. E.g., for a magnetic field of 500 G the energy of electrons whose critical frequency is 2 THz is 16 MeV. FIR measurements appear then as a unique tool to study the ability of flares to accelerate electrons to such high energies, the elementary time scales of acceleration, and the frequency of such events.

From the previous section, it is clear that measurement of the size of the emitting region and of the spectrum in the FIR domain constitute unique tools to determine if the upturn of the radio spectrum observed in the 200-400 GHz region is due to thermal or non thermal emission, and, in the latter case, which emission process is the most likely. among the various mechanisms that have been proposed so far. The identification of the radiation process is necessary to determine the physical parameters (temperature, electronic density, magnetic field,...) of the emitting source, the nature (electrons, positrons or protons) of the radiating particles as well as their characteristics (numbers, energy spectra).

In summary imaging and photometric observations of the FIR continuum during flares constitute key measurements that may involve novel physics and that may put new and stringent constraints on particle acceleration processes and models.

3.2. Structure and dynamics of the flaring atmosphere

As emphasized in the introduction, the FIR continuum is the best known thermometer throughout most of the photosphere and the chromosphere so that it has played an important role in deriving atmospheric models of the quiet solar atmosphere (Deming et al. 1991). We have shown above that during the gradual phase of flares an excess above the quiet thermal emission is observed at submillimeter wavelengths. The time profile of the 210-345 GHz radio emission in Fig. 3 shows that the slowly varying emission, which is predominant during the gradual phase, started quasi simultaneously with the impulsive phase suggesting that thermal emission from the flaring atmosphere may also be present during the impulsive phase. Based on semi-empirical models of the flaring atmosphere Heinzel & Avrett (2012) have shown that there may be a significant excess of FIR continuum during this extended flare phase. Furthermore the FIR continuum being radiated by free-free emission, the radiative transport is much simpler than for UV or optical lines which need non-LTE analysis. Time dependent photometric observations of the FIR continuum at several wavelengths appear as the most powerful way to derive the temperature and density structure of the lower solar atmosphere during flares as well as its dynamics.

3.3. Energy transport

It is well documented that flare energy is released in the corona and subsequently transported to the underlying atmosphere. Several mechanisms have been envisioned: conduction

(mediated by shock front), radiative warming, and transport by energetic particles (electrons or ions). Comparison of high cadence (< 1 s) hard X-ray and imaging observations in an optical chromospheric line (usually Hα) have been occasionally used to identify the energy transport process(es) at work during a flare. For example Trottet et al. (2002) reported a flare for which both conduction and beams of energetic electrons play a role, either of them dominating in different epochs of the flare. Here again, the thermal bremsstrahlung at FIR wavelengths is expected to be more easily amenable to quantitative interpretation than the optical and UV lines of atoms and ions.

4. Concepts for flare observations at THz frequencies

Due to strong absorption by the terrestrial atmosphere much of the FIR spectrum is not accessible from ground. Up to now two exploratory instrumental concepts have been proposed to perform observations of flares in the FIR continuum: DESIR and SOLAR T.

DESIR (Detection of Eruptive Solar InfraRed emission) is a two-bandwidth radiometer which provides full-disk observations of the Sun in the far infrared domain. The instrument images the solar disk on two detectors in the spectral bands [25 - 45 μm, 12 -6.7 THz] and [80 -130 μm, 3.75 - 2.3 THz], after spectral selection and splitting. DESIR is an un-cooled instrument using thermal detectors (commercial micro-bolometer matrices adapted to work in both wavelength bands). The minimum flux density that DESIR could detect is of 10^{-18} Wm^{-2}Hz^{-1} (10^4 sfu) at a time cadence of ten frames per second. DESIR also provides the locations of the FIR emitting regions with a spatial resolution of ∼ 50″at 35 μm. The design of DESIR was developed at LESIA/Observatoire de Paris in the framework of the SMESE (SMall Explorer for Solar Eruptions) micro-satellite project Vial et al. (2008). SMESE was declared ready for a phase B study by CNES, but not continued for programmatic and financial reasons.

The Solar T instrument comprises two 76 mm diameter telescopes designed to observe the whole solar disk at 3 and 7 THz (Kaufmann et al. 2012). The detectors are Golay cells preceded by low-pass filters to suppress visible and near IR radiation, bandpass filters around 3 and 7 GHz, and choppers. In principle, Solar T can detect temperature variations smaller than 1 K with time resolution of a fraction of a second. A laboratory photometer prototype has been developed. The experiment is planned to fly aboard stratospheric balloons, coupled to the GRIPS gamma-ray experiment (Shih et al. 2012) in cooperation with University of California, Berkeley, US. One engineering flight over USA and a two weeks flight over Antarctica are scheduled respectively for Fall 2013 and 2014-2015 Austral Summer. Another long duration stratospheric balloon flight over Russia (one week) in cooperation with the Lebedev Physics Institute, Moscow is also envisaged for 2015- 2016.

5. Conclusion

This report has presented a brief overview of 200-400 GHz observations of flares, the understanding of which need measurements of the continuum emission at higher frequencies including the FIR (1-20 THz) continuum. It has been shown that such measurements will bring new diagnostics of high-energy particles accelerated during solar flares and stringent constraints on acceleration mechanisms. They may contain novel physics of emission processes at work in the THz domain. They also constitute a unique way to quantitatively study the structure and dynamics of the low flaring atmosphere as well as energy transport processes from the corona to the chromosphere. Below 1 THz, the Atacama Large Millimeter Array (ALMA, Loukitcheva, Solanki & White (2008)) offers an interesting possibility to combine excellent image quality and high spatial resolution. In the FIR domain the detector technology is rapidly evolving. This will open the possibility to envisage future instruments with higher sensitivities, and better spectral and imaging capabilities than DESIR and Solar T. Furthermore, it is necessary to obtain joint FIR, hard X-ray, gamma-ray, and UV/EUV spectral and imaging measurements in order to

provided an overall picture of particle acceleration and energy transport during flares which puts the new findings from the FIR diagnostics into their context. The comparison with the observations of STIX on Solar orbiter (Hurford el al. 2010) may bring partial answers but lacks of high-energy gamma-ray measurements. We thus emphasize that a solar dedicated mission concept, similar to the SPARK concept proposed to ESA by Matthews et al. (2012), combining all required measurements from the FIR domain to high-energy gamma-rays is needed to fully achieve the scientific objectives mentioned above.

References

Bastian, T. S., Benz, A. O., & Gary, D. E. 1998, ARA&A, 36, 131

Costa, J. E. R., & Simões, P. J. A. 2006, IAU, Joint Discussion, vol. 1

Degiacomi C. G., et al. 1985, ApJ, 298, 918

Deming, D., et al. 1991, in A. Cox, W. Livingston, M. Matthews (eds), *Solar interior and atmosphere*, Tucson, AZ, University of Arizona Press, p.933-963

Fleishman, G. D., & Toptygin, I. N. 2007, MNRAS, 381, 1473

Fleishman, G. D., & Kontar, E. P. 2010, ApJ, 709, L127

Giménez de Castro, C. G. 2009, A&A, 507, 433

Heinzel, P., & Avrett, E. H. 2012, Solar Phys., 277, 31

Hurford, G. J., et al. 2010, AAS Abstracts, 216 #404.16

Kaufmann, P., et al. 1986, A&A, 157, 11

Kaufmann, P., et al. 2001, in Brekke, P. Fleck, B. & Gurman, J. B., *Recent Insights into the Physics of the Sun and Heliosphere: Highlights from SOHO and Other Space Missions*, IAU Symposium, 203, 283

Kaufmann, P., et al. 2004, ApJ, 603, L121

Kaufmann, P., et al. 2009, Solar Phys., 255, 131

Kaufmann, P., et al. 2012, SPIE Conference Series, 8442

Kaufmann, P., & Raulin, J.-P. 2006, Physics of Plasmas, 13, 701

Krucker, S., et al. 2012, A&AR, submitted

Louarn, P., Le Queau, D., & Roux, A. 1987, Solar Phys., 111, 201

Loukitcheva, M. A., Solanki, S. K., & White, S. M. 2008, APSS, 313, 1997

Lüthi, T., et al. 2004a, A&A, 415, 1123

Lüthi, T., et al. 2004b, A&A, 420, 361

Matthiews, S. A., et al. 2012, Experimental Astronomy, 33, 237

Ohki, K. & Hudson H. S. 1975, Solar Phys., 43, 405

Pacholczyk, A. G. 1970, *Radio Astrophysics*, San Francisco: W. H. Freeman & Co

Pick, M., Klein, K.-L., & Trottet, G. 1990, ApJS, 73, 165

Sakai, J. I., & Nagasugi, Y. 2007a, A&A, 474, L33

Sakai, J. I., & Nagasugi, Y. 2007b, A&A, 470, 1117

Sakai, J. I. et al. 2006, A&A, 457, 313

Shih A., Y., et al. 2012, SPIE Conference Series, 8443

Silva, A. V. R., et al. 2007, Solar Phys., 245, 311

Trottet G., et al. 2000, A&A, 356, 1067

Trottet G., et al. 2002, A&A, 381, 694

Trottet G., et al. 2008, ApJ, 678, 509

Trottet G., et al. 2011, Solar Phys., 273, 339

Vial, J. C., et al. 2008, AdSpR, 41, 183

White, S. M., & Kundu, M. R. 1992, Solar Phys., 141, 347

Wu, C. S. 1985, Space Science Reviews, 41, 215